社団法人 情報処理学会 研究報告
IPSJ SIG Technical Report

2006－CVIM－153 (10)
2006／3／16

視覚ポテンシャルによるロボットナビゲーション

大西 直哉† 井宮 淳††

† 千葉大学大学院自然科学研究科
†† 千葉大学総合メディア基盤センター
〒263-8522 千葉市稲毛区弥生町 1-33
E-mail: †ohnishi@graduate.chiba-u.jp, ††imiya@media.imit.chiba-u.ac.jp

あらまし 本論文では、視覚ポテンシャルを用いた移動ロボットのナビゲーション法を提案する。視覚ポテンシャルは、カメラを搭載したロボットが移動することで得られる画像列とオプティカルフローから計算される。本アルゴリズムは、環境に対する事前知識を用意しておかなくても、障害物に衝突することなく移動ロボットを行動させることができる。シミュレーション画像と実画像を用いた実験より、本アルゴリズムがロボットの初期位置や移動に対する誤差にロバストであることを示す。
キーワード ポテンシャル法, オプティカルフロー, 障害物回避

Robot Navigation by Visual Potential

Naoya OHNISHI† and Atsushi IMIYA††

† School of Science and Technology, Chiba University
†† Institute of Media and Information Technology, Chiba University
Yayoicho 1-33, Inage-ku, 263-8522, Chiba, Japan
E-mail: †ohnishi@graduate.chiba-u.jp, ††imiya@media.imit.chiba-u.ac.jp

Abstract In this paper, we aim to develop an algorithm for navigation of an autonomous mobile robot using a visual potential. The visual potential is computed from an image sequence and optical flow observed through a vision system mounted on the mobile robot. Our algorithm enables mobile robots to avoid obstacles without any knowledge on a robot workspace. We demonstrate some experimental results using image sequence observed by a moving camera in a simulated environment and a real environment. We also show that our algorithm is robust against the fluctuation of a displacement and configuration of a mobile robot.
Key words potential field, optical flow, collision avoidance

1. Introduction

In this paper, we develop a navigation algorithm for an autonomous robot using potential field method. Path planning is a problem to derive optimal or sub-optimal path from a start to a destination using the map of robot-work space which is called configuration space and landmarks [1] [2]. Navigation is a problem to derives optimal direction to move form a sequence of snap-shot of obstacle configuration in robot work space [3] [4]. A potential field method computes a path from a start to a destination using gradient field computed from potential field derived by the map of robot workspace configuration [5] [6] [7]. For the path planning by potential method, a robot is required to store the map of robot work space. In this scene potential field method for path planning is a model-based robot control. The potential field method determine the navigation path using the repulsive force from obstacles in a map, the attractive force from the start and the repulsive force to the destination, as shown in Fig.1. However, this method is invalid for the navigation when the robot does not have an environmental map. Additionally, in the real environment, it is difficult to determine the current position of the robot in an environmental map. For navigation, we are required to design non-model-based or featureless control strategy. Therefore we develop a method for consistent local potential field from a small collection of observations. In the previous paper [8], we developed a featureless robot navigation method based on optical flow computed from a pair of successive images. This method also constructs local obstacle maps by detecting the dominant plane in images.

In this paper, we introduce a visual potential field, which is computed from an potential field in an image and optical flow [9] [10] [11] [12] observed through a vision system mounted on the mobile robot. Using the visual potential field and optical flow, we define a control flow for robot navigation to avoid collision with obstacles, as shown in Fig.2.

In section 2, we briefly overview our featureless method for detection of the dominant plane using optical flow. Section 3 is devote for the introduction of visual potential field and definition of control force computed from the visual field. In section 4, we show some experimental results for the robot navigation.

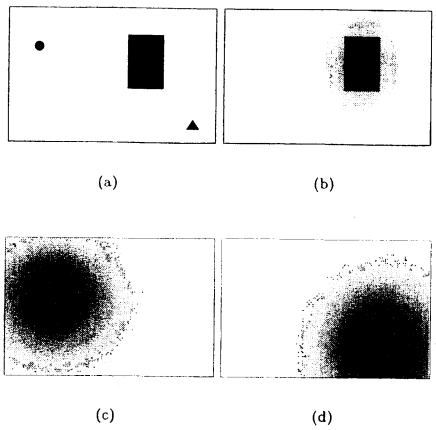

(a) (b)

(c) (d)

Fig. 1 Configuration of the obstacle and start and destination points. (a)The circle and the triangle and the rectangle are the start, the destination, and the obstacle. (b)The repulsive force from the obstacle. (c)The attractive force from the start. (d)The repulsive force to the destination.

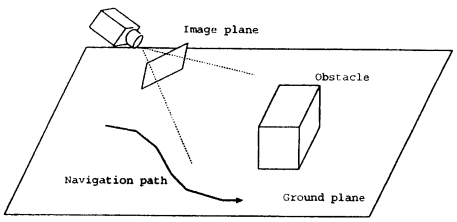

Fig. 2 Configuration of robot workspace. Our method derives the navigation path without collision with obstacles without require the environmental map.

2. Dominant Plane Detection from Optical Flow

In this section, we briefly describe the algorithm for dominant plane detection using optical flow observed through a camera mounted on a mobile robot. The detail of our algorithm is described in [8]. We define that the dominant is the largest planar domain in a scene.

We set $\boldsymbol{u}(x, y, t)$ to be the optical flow computed from successive images at time t and $t-1$. If a point (x, y) belongs to the dominant plane of the image, the relationship

$$A\boldsymbol{u}(x, y, t) + \boldsymbol{b} = 0, \tag{1}$$

are approximately satisfied [13], where A and $\boldsymbol{b}$ are the 2×2 matrix and two-dimensional vector, respectively.

If the matrix A and the vector $\boldsymbol{b}$ are obtained

$$\hat{\boldsymbol{u}}(x, y, t) = -A^{-1}\boldsymbol{b}, \tag{2}$$

represents the dominant plane motion in the successive images. We express the flow $\hat{\boldsymbol{u}}(x, y, t)$ as *planar flow*.

Since the planar flow $\hat{\boldsymbol{u}}(x, y, t)$ is equal to the optical flow $\boldsymbol{u}(x, y, t)$ on the dominant plane, we use the difference between these two flows. Setting ε to be the tolerance of the

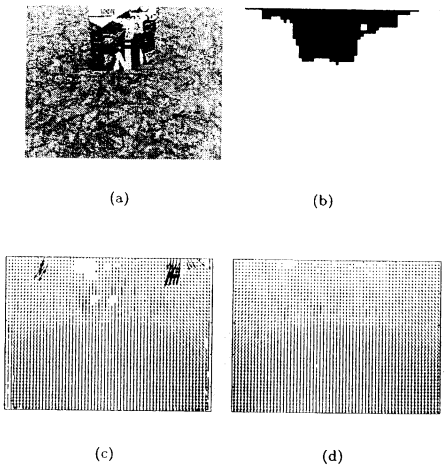

(a) (b)

(c) (d)

Fig. 3 Example of the dominant plane. (a)Image. (b)Detected dominant plane $d(x, y, t)$. The white areas are the dominant planes, and the black areas are obstacles. (c)Optical flow $\boldsymbol{u}(x, y, t)$. (d)Planar flow $\hat{\boldsymbol{u}}(x, y, t)$.

difference between the optical flow vector and the planar flow vector, if

$$|\boldsymbol{u}(x, y, t) - \hat{\boldsymbol{u}}(x, y, t)| < \varepsilon, \tag{3}$$

is satisfied, we accept the point (x, y) as the point in the dominant plane. We set $d(x, y, t)$ to be the dominant plane, as

$$d(x, y, t) = \begin{cases} 255 & \text{for Dominant Plane} \\ 0 & \text{for Obstacle Area} \end{cases} \tag{4}$$

For the computation of the matrix A and the vector $\boldsymbol{b}$ from the optical flow which contain the dominant plane and obstacles area, we use RANSAC method. Our algorithm is summarized as follows:

(1) Compute optical flow $\boldsymbol{u}(x, y, t)$ from two successive images.

(2) Compute affine coefficients in Eq.(1) by random selection of three points.

(3) Estimate planar flow $\hat{\boldsymbol{u}}(x, y, t)$ from affine coefficients.

(4) Matching the computed optical flow $\boldsymbol{u}(x, y, t)$ and estimated planar flow $\hat{\boldsymbol{u}}(x, y, t)$ by using Eq.(3).

(5) Detect the dominant plane. If the dominant plane occupies less than half of the image, then go to step(2).

Figure 3 shows the examples for the image, the detected dominant plane, the optical flow and the planar flow

3. Determination of the robot motion using Visual Potential

In this section, we develop an algorithm for the determination of a robot motion in the direction form the dominant plane image $d(x, y, t)$ and the planar flow $\hat{\boldsymbol{u}}(x, y, t)$.

3.1 Gradient Vector of Image Sequence

A robot moves on the dominant plane without collision with obstacles. Therefore, we generate a repulsive force form

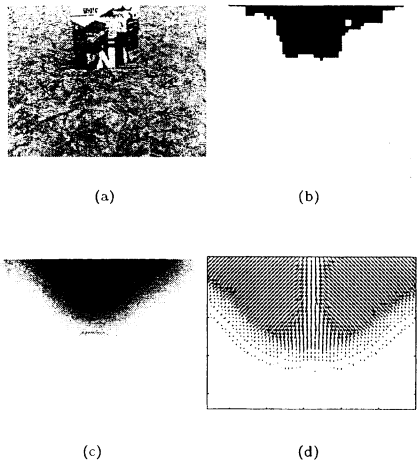

Fig. 4 Example of the gradient vector field. (a)Image. (b)Detected dominant plane $d(x,y,t)$. (c)Gaussian operator $G * d(x,y,t)$. (d)Gradient vector field $\boldsymbol{g}(x,y,t)$.

the obstacles area in the image $d(x,y,t)$ using a gradient vector field. We set $\boldsymbol{g}(x,y,t)$ to be the gradient vector field of the dominant plane $d(x,y,t)$,

$$\boldsymbol{g}(x,y,t) = \nabla(G * d(x,y,t)) = \begin{pmatrix} \frac{\partial}{\partial x}(G * d(x,y,t)) \\ \frac{\partial}{\partial y}(G * d(x,y,t)) \end{pmatrix} \quad (5)$$

where $G*$ is a gaussian operator to compute smoothly the gradient vector field. The example for the gradient vector field is shown in Fig.4.

3.2 Optical Flow as an Attractive Force

The gradient vector field $\boldsymbol{g}(x,y,t)$ is a repulsive force from obstacles. Then, we use the planar flow $\hat{\boldsymbol{u}}(x,y,t)$ as an attractive force. Since the plan flow $\hat{\boldsymbol{u}}(x,y,t)$ represents the camera motion, the sum of the sign-inversed planar flow $-\hat{\boldsymbol{u}}(x,y,t)$ and the gradient vector field $\boldsymbol{g}(x,y,t)$ is the potential field $\boldsymbol{p}(x,y,t)$. However, in the obstacles area in an image, the planar flow $\hat{\boldsymbol{u}}(x,y,t)$ is set to 0, since the planar flow represents the dominant plane motion. Therefore, we define potential field $\boldsymbol{p}(x,y,t)$ is

$$\boldsymbol{p}(x,y,t) = \begin{cases} \boldsymbol{g}(x,y,t) - \hat{\boldsymbol{u}}(x,y,t) & \text{where } d(x,y,t) = 255 \\ \boldsymbol{g}(x,y,t) & \text{where } d(x,y,t) = 0 \end{cases} \quad (6)$$

The example for the potential field $\boldsymbol{p}(x,y,t)$ is shown in Fig.5 computed from the examples in Fig.4.

3.3 Navigation from Potential Field

Using the potential field $\boldsymbol{p}(x,y,t)$, we determine the robot motion. We define that the mean value of $\boldsymbol{p}(x,y,t)$ in the image,

$$\bar{\boldsymbol{p}}(t) = \frac{\sum_{x,y} \boldsymbol{p}(x,y,t)}{\sum_{x,y} 1} \quad (7)$$

is the control force. We set a parameter $theta(t)$ to be the angle between the front of the mobile robot and the control force $\boldsymbol{p}(x,y,t)$, as shown in Fig.6. We define that the robot displacement $T(t)$ and rotation $R(t)$ at time t are

$$T(t) = T_m \cos\theta(t), \quad (8)$$

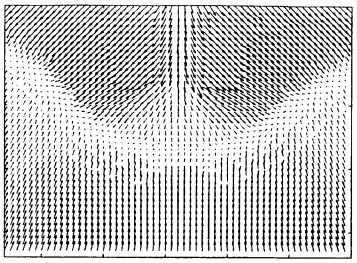

Fig. 5 Example for potential field $\boldsymbol{p}(x,y,t)$ computed from the examples in Fig.4.

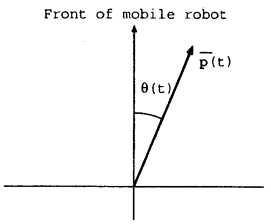

Fig. 6 The angle between the front of the mobile robot and the control force $\boldsymbol{p}(x,y,t)$ is a parameter $theta(t)$.

$$R(t) = R_m \sin\theta(t), \quad (9)$$

where T_m and R_m are the maximum displacement and the rotation of the mobile robot between t and $t+1$.

4. Experimental Results

In this section, we show some experimental results for autonomous robot navigation.

4.1 Experiments using real image sequence

Figure 7 shows experimental results for estimation of visual potential and the control force. In Fig.7, starting from the left, images show the configuration of the robot and obstacles, the captured image, the detected dominant plane $d(x,y,t)$, the gradient vector field $\boldsymbol{g}(x,y,t)$, the potential field $\boldsymbol{p}(x,y,t)$, and the estimated control force $\bar{\boldsymbol{p}}(t)$. For the computation of optical flow, we use the Lucas-Kanade method with pyramids [14].

4.2 Experiments in synthetic environment

Mobile robots in a real environment have errors against the fluctuation of a displacement and configuration of the robots. Therefore, we create synthetic environmental maps for the evaluation of the robustness of our method against these errors. Figure 8(a) shows an environmental map. In this map, The triangle is an initial position of the mobile robot. And Fig.8(b) is the estimated navigation path using our method.

We assume that the robot has the errors with 20% against a robot displacement $T(t)$ and rotation $R(t)$ in Eq.9, as shown in Fig.9. Additionally, we added the error with 20% against estimated dominant plane $d(x,y,t)$, as shown in Fig.10. The result of the experiment with these errors are shown in Fig11.

Figures 12 and 13 show the experimenatl results using another environmental maps.

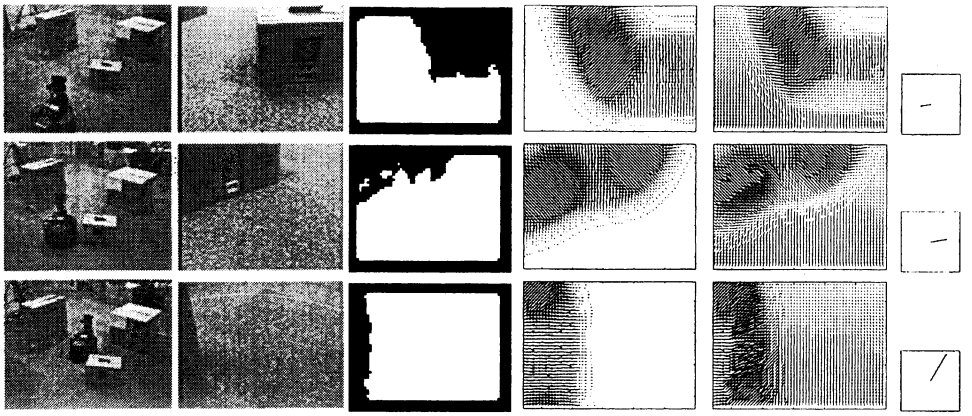

Fig. 7 Experimental results for estimation of visual potential. Starting from the left, images show the configuration of the robot and obstacles, the captured image, the detected dominant plane $d(x, y, t)$, the gradient vector field $\boldsymbol{g}(x, y, t)$, the potential field $\boldsymbol{p}(x, y, t)$, and the estimated control force $\bar{\boldsymbol{p}}(t)$.

5. Conclusion

we developed a navigation algorithm for an autonomous robot using visual potential field. Our method enable a mobile robot to avoid obstacles without require the environmental map. Experimental results show that our algorithm is robust against the fluctuation of a displacement and configuration of a mobile robot.

Reference

[1] Guilherme, N. D. and Avinash, C. K., Vision for mobile robot navigation: A survey, IEEE Trans. on PAMI **24**, 237-267, (2002).

[2] Trihatmo, S. and Jarvis, R.A., Short-safe compromise path for mobile robot navigation in a dynamic unknown environment, Australian Conference on Robotics and Automation (2003).

[3] Conner, D.C., Rizzi, A.A., and Choset, H., Composition of local potential functions for global robot control and navigation, Proceedings of 2003 IEEE/RSJ International Conference on Intelligent Robots and Systems, **4**, pp.3546–3551, (2003).

[4] Tews, A.D., Sukhatme, G.S., and Matarić M.J,, A multi-robot approach to stealty navigation in the presence of an observer, ICRA 2004, 2379–2385, (2004).

[5] Shimoda, S., Kuroda, Y., and Iagnemma, K., Potential Field Navigation of High Speed Unmanned Ground Vehicles on Uneven Terrain. ICRA 2005, 2839–2844, (2005).

[6] Valavanis K, Hebert T., Kolluru R., and Tsourveloudis N., Mobile robot Navigation in 2D dynamic Environments using an Electrostatic Potential Field, IEEE Transactions on systems, man, and cybernetics, **30**, 187–196, (2000).

[7] Aarno, D., Kragic, D., and Christensen, H.I., Artificial Potential Biased Probabilistic Roadmap Method, ICRA 2004, **1**, 461–466, (2004).

[8] Ohnishi, N. and Imiya, A., Featureless robot navigation using optical flow, Connection Science Vol.17, pp.23-46, (2005).

[9] Barron, J.L., Fleet, D.J., and Beauchemin, S.S., Performance of optical flow techniques, International Journal of Computer Vision, **12**, 43-77, (1994).

[10] Horn, B. K. P. and Schunck, B.G., Determining optical flow, Artificial Intelligence, **17**, 185-203, (1981).

[11] Lucas, B. and Kanade, T., An iterative image registration technique with an application to stereo vision, Proc. of 7th IJCAI, 674-679, (1981).

[12] Nagel, H.-H. and Enkelmann, W., An investigation of smoothness constraint for the estimation of displacement vector fields from image sequences, IEEE Trans. on PAMI, **8**, 565-593, (1986).

[13] Hartley, A. and Zisserman, A., *Multiple View Geometry in Computer Vision*, Cambridge University Press, (2000).

[14] Bouguet J.-Y., Pyramidal implementation of the Lucas Kanade feature tracker description of the algorithm, Intel Corporation, Microprocessor Research Labs, OpenCV Documents, (1999).

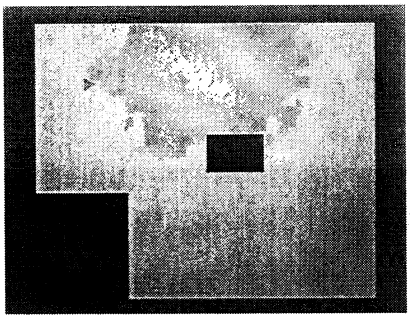

(a)

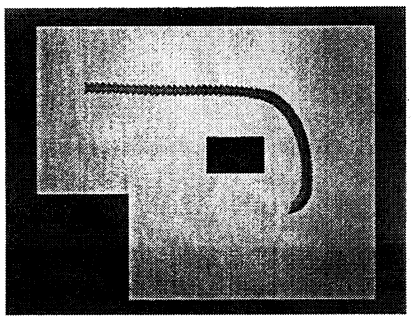

(b)

Fig. 8 Environmental map. (a)The triangle in the map is an initial position of the mobile robot. The black coloured regions are obstacles. (b)Computed navigation path without any errors.

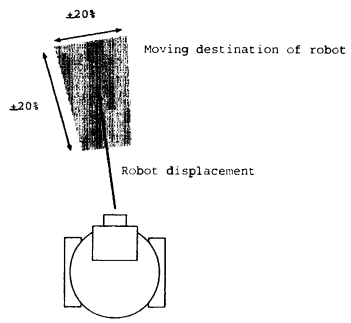

Fig. 9 The mobile robot has an error against a displacement. The error with 20% was added to a robot displacement $T(t)$ and rotation $R(t)$.

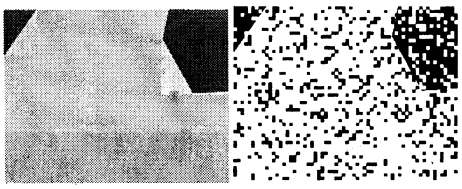

(a) (b)

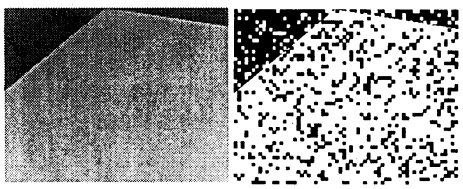

(c) (d)

Fig. 10 The examples of the error against estimated dominant plane $d(x, y, t)$. (a)(c)Original images. (b)(d)Images that error with 20% was added to (a) and (c), respectively.

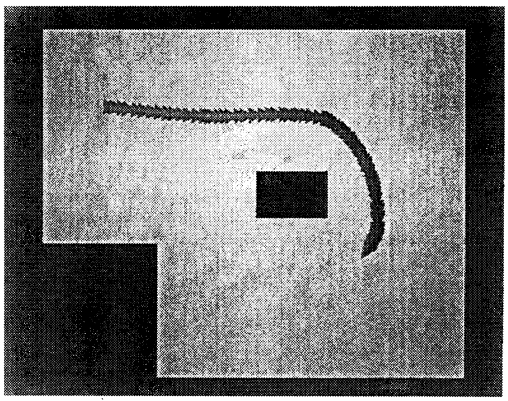

Fig. 11 Computed navigation path with errors against a displacement and dominant plane detection.

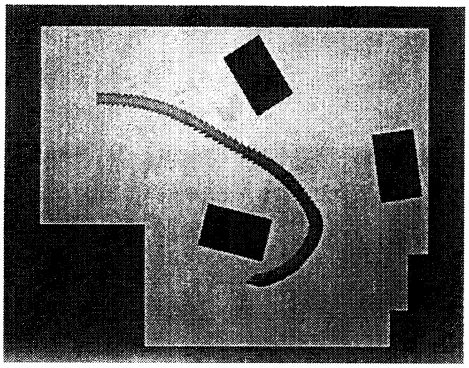

(a)

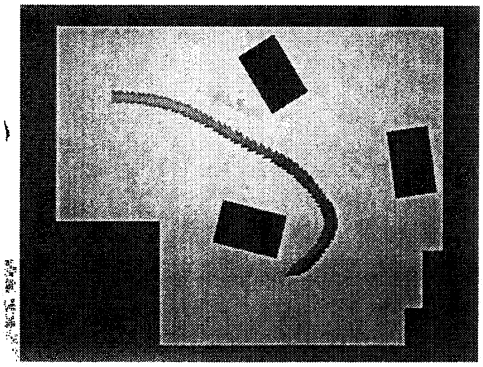

(b)

Fig. 12 (a)Computed navigation path without any errors. (b)Computed navigation path with errors against a displacement and dominant plane detection.

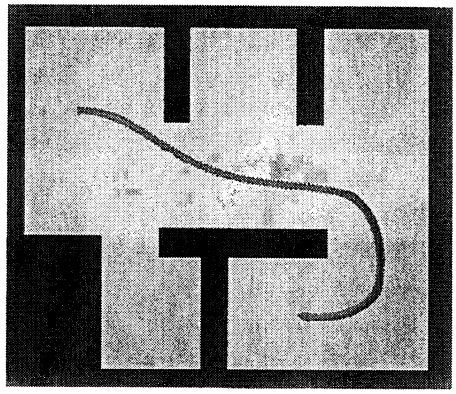

(a)

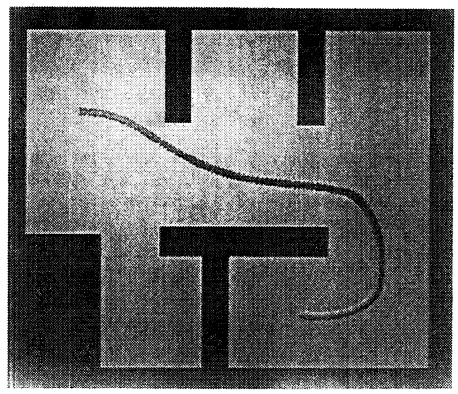

(b)

Fig. 13 (a)Computed navigation path without any errors. (b)Computed navigation path with errors against a displacement and dominant plane detection.